AIAA JOURNAL
Vol. 38, No. 1, January 2000

Strength Prediction of Fiber Reinforced Plastics with a Hole Under Compression–Tension

C. Soutis,* C. Filiou,† and V. Pateau‡
Imperial College of Science, Technology, and Medicine, London, England SW7 2BY, United Kingdom

An approximate solution in the form of a polynomial is developed for the in-plane stresses near a circular hole in an orthotropic composite laminate under biaxial loading. The derived stresses are found to be in good agreement with the exact anisotropic solution for a series of laminates investigated. However, the degree of accuracy of the approximate stress distribution is strongly influenced by the laminate layup and the biaxiality ratio. The resultant stresses are then employed in a fracture mechanics model to estimate the damage initiation, growth, and final fracture of carbon fiber–epoxy plates with an open hole subjected to biaxial compression–tension static loading. Using the independently measured laminate parameters of unnotched strength and in-plane fracture toughness, the model successfully predicts the notched strength of multidirectional laminates under various biaxiality ratios.

Introduction

THE uniaxial tensile or compressive behavior of composite laminates with an open hole have been given considerable attention in the literature.[1,2] However, very few studies[3,4] have been reported for the evaluation of the notched strength of laminates under biaxial loading. Strength prediction methods have been almost entirely limited to uniaxial loading. Daniel[5] extended the average stress failure criterion, developed by Whitney and Nuismer[6] for uniaxial tensile loading, to solve the problem of a quasi-isotropic notched laminate under equibiaxial tensile stress; the method was complex and did not result in a simple solution suitable for use in design.

In the present paper, the Soutis–Fleck model[7] (see also Ref. 8) is modified to predict the notched strength of carbon fiber reinforced plastic (CFRP) laminates under tension–compression loading, where final failure is due to 0-deg fiber microbuckling; the 0-deg plies are parallel to the compression load. The model is based on the stress intensity factor K_I for cracks emanating symmetrically from the edge of the hole and the stress distribution adjacent to the hole. The latter can be calculated by using either analytical or computational (finite element) methods. The stress distribution near a circular hole, in orthotropic plates under biaxial in-plane loading, has been examined analytically[9,10] and is based on the complex variable mapping approach.[11–14] However, this solution is cumbersome to apply without the use of an electronic computer. In this work, a simple polynomial expression for the stress distribution is described and compared with the exact one. It is based on the limiting characteristics of the exact solution and is an extension of the polynomial expression developed by Konish and Whitney[15] for the uniaxial loading case. The new expression is then employed with the Soutis–Fleck[7] fracture model to examine the notch sensitivity of CFRP plates under biaxial compressive-dominated loading; predictions are compared to experimental data.

Derivation of the Approximate Solution

The problem of interest consists of an open circular hole extending through the thickness of an orthotropic composite laminate under biaxial loading (see Fig. 1). The in-plane dimensions of the plate are very large compared to the hole diameter, and the material is assumed to be homogeneous, elastic, and anisotropic, corresponding to the lamination theory model of a midplane symmetric fiber composite laminate.

Konish and Whitney[15] derived an approximate solution in the form of a polynomial for the normal stress distribution adjacent to a circular hole in an infinite orthotropic plate under uniaxial loading. The polynomial is obtained by adding sixth- and eighth-order terms to the isotropic stress solution, that is,

$$\sigma_{xx}^{\text{orth}}(0, y)/p = 1 + \tfrac{1}{2}\xi^{-2} + \tfrac{3}{2}\xi^{-4} + f(\xi) \tag{1}$$

For the biaxial load case (Fig. 1) the stress distribution can be written as

$$\sigma_{xx}^{\text{orth}}(0, y)/p = 1 + [(\lambda + 1)/2]\xi^{-2} + [3(1 - \lambda)/2]\xi^{-4} + f(\xi) \tag{2}$$

where $\xi = y/R$, with R the hole radius, λ the biaxiality ratio (q/p), and

$$f(\xi) = a\xi^{-6} + b\xi^{-8} \tag{3}$$

Although there is no unique form for $f(\xi)$, some general properties of this function may be deduced. Because the problem of interest is symmetric with respect to the x axis, $f(\xi)$ must be symmetric with respect to its argument. Furthermore, it is clear that $f(\xi)$ must approach zero as ξ increases without limit because both isotropic and anisotropic stresses must approach a common limit at large ξ. The a and b coefficients are determined by requiring the exact value of the stress concentration factor (SCF) to be recovered at the hole boundary and requiring that overall balance of force resultants be obtained.

We first evaluate Eq. (2) at the hole boundary ($\xi = y/R = 1$), obtaining the SCF at point A:

$$K_A^{\text{orth}}(0, R) = K_A^{\text{iso}} + f(\xi = 1) \tag{4}$$

where $K_A^{\text{iso}} = 3 - \lambda$. By the substitution of Eq. (3) and rearranging, Eq. (4) becomes

$$a + b \cong K_A^{\text{orth}} - (3 - \lambda) = [H_A - 1]K_A^{\text{iso}} \tag{5}$$

with $H_A = (K_A^{\text{orth}}/K_A^{\text{iso}})$; this parameter measures the magnitude of the orthotropic effect. The orthotropic stress concentration factor at point A of the hole boundary due to loads p and q is given by Lekhnitskii[11] as

$$K_A^{\text{orth}} = 1 + n - \lambda k \tag{6}$$

where

$$k = \sqrt{E_{xx}/E_{yy}}, \qquad n = \sqrt{2\left(\sqrt{E_{xx}/E_{yy}} - \nu_{xy}\right) + E_{xx}/G} \tag{7}$$

Presented as Paper 98-1701 at the AIAA/ASME/ASCE/AHS/ASC 39th Structures, Structural Dynamics, and Materials Conference, Long Beach, CA, 20–23 April 1998; received 10 July 1998; revision received 4 May 1999; accepted for publication 16 June 1999.

*Reader in Mechanics of Composites, Department of Aeronautics, Prince Consort Road.
†Research Associate, Aeronautics Department.
‡Research Assistant, Aeronautics Department.

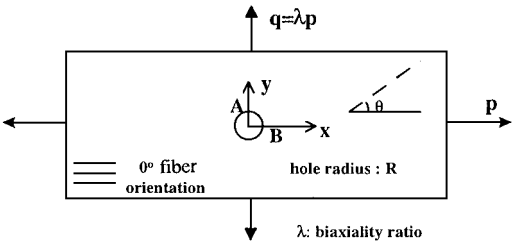

Fig. 1 Orthotropic open-hole plate subjected to biaxial loading.

with E, G, and ν being the laminate elastic properties in x–y Cartesian coordinates.

A second equation for a and b is obtained by requiring that the force resultants of both the exact and approximate anisotropic stress distributions be equal, that is,

$$\int_R^\infty \left[\frac{\sigma_{xx}^{\text{orth}}(0, y)}{p}\right] dy = \int_R^\infty \left[\frac{\sigma_{xx}^{\text{iso}}(0, y)}{p}\right] dy + \int_R^\infty f\left(\xi = \frac{y}{R}\right) dy \tag{8}$$

Additionally, the total force of the isotropic stress distribution must be equal to the force resultant of the anisotropic exact stress distribution because both stress resultants must be in equilibrium with the resultant of a single applied loading. Thus,

$$\int_R^\infty \left[\frac{\sigma_{xx}^{\text{orth}}(0, y)}{p}\right] dy = \int_R^\infty \left[\frac{\sigma_{xx}^{\text{iso}}(0, y)}{p}\right] dy \tag{9}$$

By the substitution of Eq. (9) for Eq. (8), it can be found that

$$\int_R^\infty f\left(\xi = \frac{y}{R}\right) dy = 0 \Rightarrow \int_1^\infty f(\xi)\, d\xi = 0$$

$$\Rightarrow \int_1^\infty (a\xi^{-6} + b\xi^{-8})\, d\xi = 0 \Rightarrow 7a + 5b = 0 \tag{10}$$

The solution of the system of Eqs. (5) and (10) leads to the determination of the a and b constants of the $f(\xi)$ polynomial. For the biaxial loading configuration shown in Fig. 1, assuming that the dominant load is on the x axis, the a and b coefficients are found as

$$\begin{aligned} a &= -\tfrac{5}{2}\left[K_A^{\text{orth}} - (3 - \lambda)\right] = -\tfrac{5}{2}K_A^{\text{iso}}[H_A - 1] \\ b &= \tfrac{7}{2}\left[K_A^{\text{orth}} - (3 - \lambda)\right] = \tfrac{7}{2}K_A^{\text{iso}}[H_A - 1] \end{aligned} \tag{11}$$

Equation (11) combined with Eqs. (2) and (3) yields the approximate stress distribution along the y axis under biaxial loading:

$$\frac{\sigma_{xx}^{\text{orth}}(0, y)}{p} \cong 1 + \frac{(\lambda + 1)}{2}\left(\frac{R}{y}\right)^2 + \frac{3(1 - \lambda)}{2}\left(\frac{R}{y}\right)^4 - (3 - \lambda)\frac{[H_A - 1]}{2}\left[5\left(\frac{R}{y}\right)^6 - 7\left(\frac{R}{y}\right)^8\right] \tag{12}$$

with $y \geq R$. Similarly, the stress distribution $\sigma_{yy}^{\text{orth}}(x, 0)$ along the x axis can be obtained:

$$\frac{\sigma_{yy}^{\text{orth}}(x, 0)}{p} \cong \lambda + \frac{(\lambda + 1)}{2}\left(\frac{R}{x}\right)^2 - \frac{3(1 - \lambda)}{2}\left(\frac{R}{x}\right)^4 - (3\lambda - 1)\frac{[H_B - 1]}{2}\left[5\left(\frac{R}{x}\right)^6 - 7\left(\frac{R}{x}\right)^8\right] \tag{13}$$

with $x \geq R$ and $H_B = (K_B^{\text{orth}}/K_B^{\text{iso}})$. The orthotropic and isotropic SCFs at point B are given by the following expressions:

$$K_B^{\text{orth}} = (1/k)[-1 + \lambda(k + n)] \tag{14}$$

$$K_B^{\text{iso}} = 3\lambda - 1 \tag{15}$$

For $\lambda = 0$ Eq. (12) reduces to that derived by Konish and Whitney[15] for the uniaxial loading case. The stress concentration factors given by Eqs. (6) and (14) depend on the proportion of the various plies in the laminate and not on the actual stacking sequence. However, the stacking sequence has a noticeable influence on the strength and failure patterns of composite laminates.

Comparison with the Exact Solution

To compare the derived approximate solution with the exact, the stress distribution in XAS/914C notched laminates under biaxial loading with the dominant load along the x axis (Fig. 1) is considered. Figures 2a–2c illustrate the extended isotropic (orthotropic)

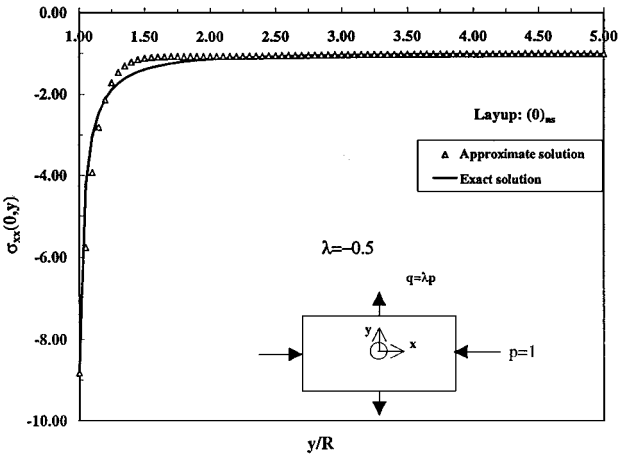

Fig. 2a Approximate and exact stress distributions for an XAS/914C open-hole laminate under biaxial loading: $(0)_{ns}$.

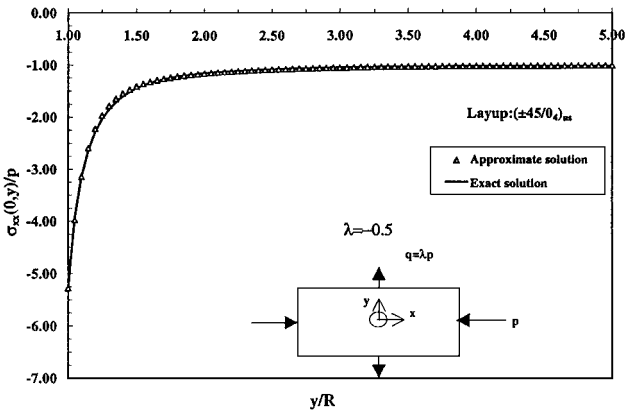

Fig. 2b Approximate and exact stress distributions for an open-hole composite plate under biaxial loading: $(\pm 45/0_4)_{ns}$.

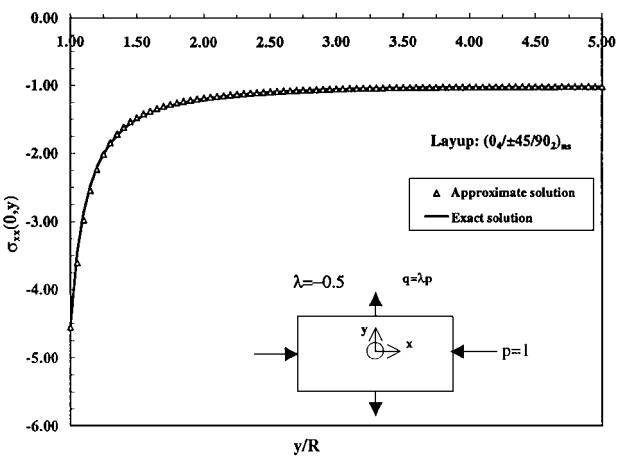

Fig. 2c Approximate and exact stress distributions for an open-hole composite plate under biaxial loading: $(0_4/\pm 45/90_2)_{ns}$.

Table 1 Maximum percentages of error for the approximate stress distribution[a]

Layup	Laminate composition[b] (±45):0:90 deg plies, %	Maximum error % occurring at $y = 1.05R$–$1.25R$			
		$\lambda = 0$	$\lambda = 0.5$	$\lambda = -0.5$	$\lambda = -1$
$[(0/90_2/0)_3]_s$	0:50:50	15	12	18	20
$[(90)_8]_s$	0:0:100	11	4	17	22
$[(\pm 45)_4]_s$	100:0:0	7	16	8	12
$(\pm 45/0_2/90_2/0_2/90_2/0_2)_s$	16.7:50:33.3	6	4	7	8
$(0_{16}/(\pm 45)_3/90_2)_s$	25:66.7:8.33	4	3	5	6
$(0_4/\pm 45/90_2)_s$	25:50:25	3	2	4	5
$[(\pm 45/0_4)_2]_s$	33.3:66.7:0	1	0	4	5
$[(\pm 45/0/90)_3]_s$	50:25:25	0	0	0	0

[a]Region $y = 1.05R$–$1.25R$, for various layups.
[b]Material under investigation is a T800/924C laminate subjected to uniaxial or biaxial loading.[10]

stress distribution σ_{xx} [Eq. (12)] and the exact solution[9,10] over a distance $y/R = 5$ from the hole boundary for a biaxiality ratio of $\lambda = -0.5$ for three layups. As expected, both solutions give the same value for the stresses developing at the hole edge (SCF). Even though some deviation of the approximate from the exact stress values can be identified, there is an overall acceptable agreement between the two stress distributions. The degree of agreement between the two stress distributions depends strongly on the layup, with the extreme cases being the unidirectional and the quasi-isotropic composite plate. Indeed, some deviation of the approximate from the exact solution is observed in the case of a laminate consisting of 100% 0-deg plies (Fig. 2). On the other hand, the presence of ±45-deg plies appears to reduce the orthotropy effect and improve the agreement of the two solutions (Figs. 2b and 2c). The effect of the higher-order polynomial terms in Eq. (12) diminishes, and the approximate expression approaches the exact isotropic solution. In general, for laminates that are dominated by off-axis plies, the error associated with the approximate solution is less than 6% (see Refs. 9 and 10). Table 1 presents the maximum error that has been recorded for the approximate stress distribution in the region $y = 1.05R$–$1.25R$ for various layups, considering that the respective laminates are subjected to uniaxial tension ($\lambda = 0$), biaxial tension–tension ($\lambda = 0.5$), and biaxial tension–compression ($\lambda = -0.5$ and -1). It can be seen that the magnitude of this error drops dramatically when ±45-deg plies are introduced in the multidirectional laminate.

Fracture Toughness Model

The derived stress distribution [Eq. (12)] can be used in any stress-based fracture model to predict the notch sensitivity and fracture behavior of composites under any biaxial loading. In the present work, the Soutis–Fleck fracture model,[7] modified to include biaxiality, is used to estimate the notched strength of XAS/914C carbon–epoxy multidirectional laminates. The original model[7] considers a multidirectional composite laminate with an open hole subjected to uniaxial compression; it employs the stress distribution at the edge of the hole and linear elastic fracture mechanics concepts. Compressive failure of such laminates is mainly due to 0-deg fiber buckling (fiber kinking) from the hole edges, accompanied by fiber–matrix debonding, matrix yielding, and delamination.[8,16–18] The microbuckle propagates initially in a stable manner along the transverse direction under increasing load. At a critical stress level it grows rapidly and catastrophic failure occurs. On a penetrant-enhanced x-ray radiograph, the microbuckled zone resembles a fatigue crack in metals. Because of its cracklike appearance, the authors[7] modeled the damage zone at the edges of the hole as a through-thickness crack (line crack) with no traction on the crack surfaces. A description of the theory is presented hereafter for the biaxial loading case.

The Soutis–Fleck model,[7] as applied to biaxial loading, is based on the following two criteria.

Stable Crack Growth

Prediction of stable crack growth is based on a critical value and the stress distribution adjacent to the circular hole. It is postulated that fiber microbuckling occurs over a distance ℓ from the hole when

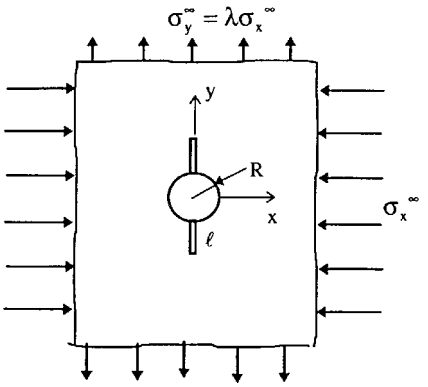

Fig. 3 Schematic representation of microbuckling (line crack) growing along the y axis under compression–tension loading.

the average stress over this distance reaches the critical stress of the unnotched laminate, σ_{un} (Fig. 3):

$$\sigma_{un} = \frac{1}{\ell}\int_R^{R+\ell} \sigma_{xx}(0, y)\,dy \tag{16}$$

where the stress distribution $\sigma_{xx}(0, y)$ is given by Eq. (12). After integration, we have

$$\sigma_{xx}^\infty = \frac{2(1-\zeta)\sigma_{un}}{(\lambda+1)(1-\zeta^2) + (1-\lambda)(1-\zeta^4) + (3-\lambda)(H_A-1)(\zeta^6-\zeta^8)} = \sigma_{un} f(R, \ell, \lambda) \tag{17a}$$

For a quasi-isotropic laminate ($H_A = 1$), Eq. (17a) reduces to

$$\sigma_{xx}^\infty = \frac{2(1-\zeta)\sigma_{un}}{(\lambda+1)(1-\zeta^2) + (1-\lambda)(1-\zeta^4)} \tag{17b}$$

where λ is the biaxiality ratio and $\zeta = R/(R+\ell)$. Microbuckling begins when $\ell = 0$ at a far-field stress σ_i^∞ given by Eq. (17a).

Experimental evidence[8,16–18] shows that in unnotched multidirectional laminates loaded in compression, failure is by 0-deg fiber microbuckling. Because of their greater axial stiffness, the 0-deg plies carry most of the load, and, hence, it is the failure of these laminae that results in laminate fracture. Therefore, by using the laminate plate theory, the model could be applied at the ply level, and the unnotched strength σ_{un} in Eq. (17a) could be replaced by the unidirectional strength σ_c^0, that is,

$$\sigma_{xx}^\infty = \sigma_c^0 g(R, \ell, E, \lambda) \tag{17c}$$

where g is a function of the hole radius R, the crack length ℓ, the laminate, and 0-deg lamina stiffness properties (represented by the variable E) and the biaxiality ratio λ.

Unstable Crack Growth

The microbuckle at the edge of the hole is assumed to behave as a crack of the same length, with no traction on the crack surfaces. Then the stress intensity factor at the tip of the crack of length ℓ from the hole edge (Fig. 3) is expressed as

$$K_I = \sigma_{xx}^{\infty}\sqrt{\pi(R+\ell)}\,Y(R,\ell,\lambda) \tag{18}$$

The length ℓ is small but finite, R is the hole radius, and σ_{xx}^{∞} is the remote applied stress. The parameter Y is a correction factor that depends on the geometry (ℓ, R), the laminate properties (orthotropy), and the biaxiality ratio. It can be obtained from a finite element analysis or analytically.[4] For a quasi-isotropic layup the Y factor can be derived from an analytical solution obtained by Newman,[19] for an isotropic open hole cracked plate under biaxial loading:

$$Y = \left\{\left[(1-\lambda)f_0\left(\frac{R}{R+\ell}\right) + \lambda f_1\left(\frac{R}{R+\ell}\right)\right]\sqrt{1-\left(\frac{R}{R+\ell}\right)}\right\} \tag{19}$$

where

$$f_0 = 1 + 0.35\left(\frac{R}{R+\ell}\right) + 1.425\left(\frac{R}{R+\ell}\right)^2 - 1.578\left(\frac{R}{R+\ell}\right)^3 + 2.156\left(\frac{R}{R+\ell}\right)^4 \tag{20}$$

$$f_1 = 1 + 0.4577\left(\frac{R}{R+\ell}\right) + 0.7518\left(\frac{R}{R+\ell}\right)^2 - 0.8175\left(\frac{R}{R+\ell}\right)^3 + 0.8429\left(\frac{R}{R+\ell}\right)^4 \tag{21}$$

Note that even though Newman[19] derived these expressions for the tension–tension loading case, the solution is still applicable to the compression–tension case because they are based on geometric parameters only. It should be remembered that the crack here is an equivalent crack representing fiber microbuckling and so crack closure is not an issue.

The model then assumes that unstable crack growth occurs when the stress intensity factor at the equivalent crack tip is equal to the laminate in-plane fracture toughness K_{IC}. The remote stress is then expressed as

$$\sigma_{xx}^{\infty} = K_{IC}/\sqrt{\pi\ell}\,Y(R,\ell,\lambda) \tag{22}$$

Using Eqs. (17) and (22), the remote stress σ_{xx}^{∞} is plotted as a function of the microbuckle length ℓ. Then the failure strength σ_n^{∞} of the notched plate is obtained from the point where the two curves intersect (Fig. 4). This point also provides the critical buckling length ℓ_{cr}. The model is formulated by assuming that the plate is of infinite width. However, small-scale laboratory test results provide notched strength data on finite-width specimens σ_n. For proper comparisons between the experimental results and predictions, the test data should be corrected into σ_n^{∞} by using an appropriate finite-width correction factor.[8,20]

The fracture mechanics approach is justified because the microbuckled zone resembles a crack and the damage zone associated with the microbuckle is small in extent compared with other specimen dimensions. The in-plane fracture toughness K_{IC} was measured[8,21] for six different T800/924C multidirectional laminates by performing a series of tests on center-cracked compression specimens. These specimens were 245 mm long by 50 mm wide with central slits perpendicular to the applied load and presharpened by a razor blade. The crack length-to-width ratios ranged from 0.1 to 0.6, and the slits were of sufficient width (about 1 mm) to prevent contact of the slit faces under compressive loading. An antibuckling device was used to prevent Euler bending, and the tests were performed on a screw-driven test machine at a displacement rate of 0.017 mm $\cdot$ s^{-1}. The specimens behaved in an elastic-brittle manner, and the fracture toughness was computed from the failure load; the orthotropic K calibration factors were obtained from a finite element analysis.[7] It was concluded that K_{IC} was independent of initial crack size and could be considered as a laminate property. Typical values for the carbon fiber–epoxy system examined were in the region of 40–50 MPa $\cdot$ m$^{1/2}$, depending on layup. For theoretical predictions of the compressive toughness and microbuckling propagation in composites, the reader should refer to some recent work by Fleck[22] and Sutcliffe and Fleck.[23] Figure 4 illustrates the effect of toughness on notch sensitivity for the biaxial loading case ($\lambda = -0.3$); the notched strength σ_n increases with increasing K_{IC}. The K_{IC} value may be influenced by the biaxaility ratio so that it would seem advisable to determine this experimentally.

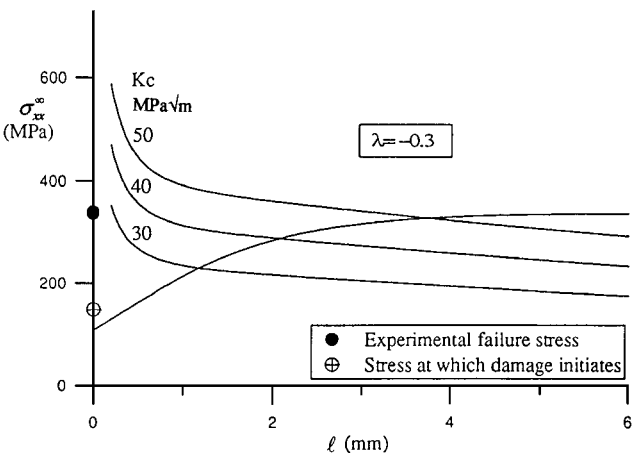

Fig. 4 Stable and unstable crack growth as a function of fracture toughness K_C; the notched strength of the XAS/914C $(+45/0/-90)_{2s}$ plate is obtained from the point where the two curves intersect.

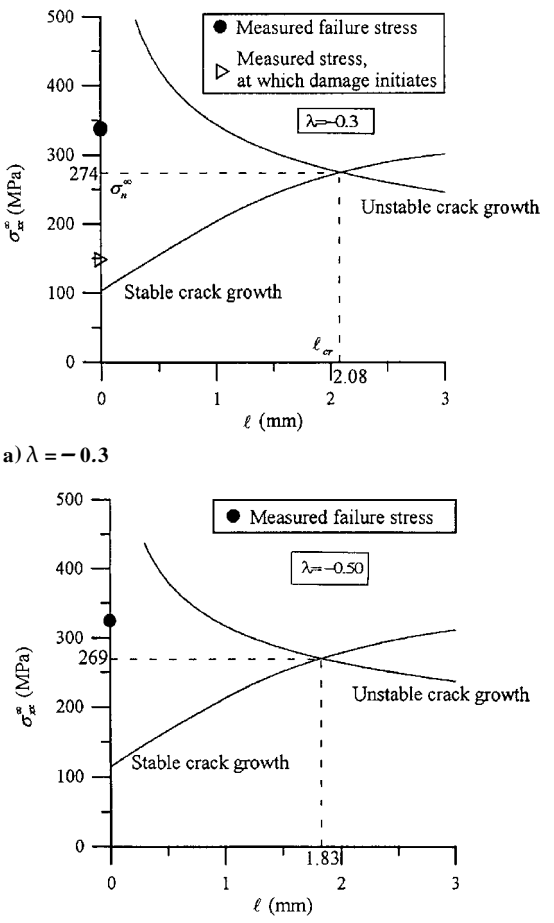

Fig. 5 Strength predictions for an XAS/914C $(+45/0/-45/90)_{2s}$ plate under compression–tension loading (W = 30 mm, R = 3 mm, and K_C = 40 MPa $\cdot$ m$^{1/2}$).

Applications

The fracture model was evaluated under uniaxial compression by Soutis,[8] and it was concluded that the effects of hole size and layup on the compressive strength can be obtained with reasonable accuracy; six T800/924C laminate stacking sequences were examined with circular holes of diameter 4–25 mm. The strength and critical microbuckle length predicted by the line-crack model were accurate to within 10% for the 0-deg-dominated laminates but less accurate for the laminate composed of mainly ±45 plies (83%). For the 45-deg-dominated layup, the model underestimated the strength by approximately 20%. The damage in this laminate is diffuse in nature, and an equivalent crack representation of damage becomes inappropriate.

To illustrate the application of the current theory to notched laminates loaded in biaxial compression–tension, some results are presented in Figs. 5a and 5b for an XAS/914C carbon–epoxy $(+45/0/-45/90)_{2s}$ quasi-isotropic laminate. The critical buckling length is about 2 mm long, and the predicted strength values for $\lambda \approx -0.3$ and -0.5 are 15–20% lower than the measured data. In these calculations, the K_{IC} value was assumed equal to 40 MPa $\cdot$ m$^{1/2}$; a higher value of K_{IC} would reduce the difference. The experimental results were obtained by testing a cruciform-type test specimen with a 30-mm square test section and a 6-mm hole diameter in a servohydraulic test machine. The damage initiation at the edge of the hole was observed by using penetrant-enhanced x-ray radiography. All specimens failed from the hole in a direction almost perpendicular to the compressive loading axis. Postfailure examination revealed that fiber microbuckling in the 0-deg plies was the dominant failure mechanism. It initiated from the hole edges and propagated across the y axis, almost perpendicular to the compression loading direction. Of course, delamination was present, but little damage occurred away from the hole, supporting the theoretical approach. Fiber microbuckling (or fiber kinking) that forms near the cutout in the 0-deg plies was also the critical failure mode observed by Khamseh and Waas[24] in composite plates loaded in biaxial compression.

The present model provides a useful predictive tool for design engineers, but it is recognized that further work is required to monitor the progressive damage development and to evaluate in more detail the effect of biaxial loading on the fracture toughness and the accuracy of the model for other laminate stacking sequences.

Conclusion

The complex nature of the exact solution for the stress distribution near the notch makes its application cumbersome; therefore, a rather simple approximate solution for biaxial loading has been introduced. This solution is based on the Konish and Whitney[15] polynomial expression developed for orthotropic plates under uniaxial loading. The extended isotropic solution yields the same stress values with the exact solution at the hole boundary. Both curves show the same general shape, and over a widely varying range of laminates and biaxiality ratios the agreement between the two solutions is acceptable.[9,10] The degree of accuracy is influenced by the layup and biaxiality ratio, and for layups containing $0/\pm45$ or $0/90/\pm45$ layers the extended isotropic solution varies from the exact by less than 6%. When the approximate stress distribution is used with the modified Soutis–Fleck model, the notched strength of an XAS/914C quasi-isotropic laminate, loaded in compression–tension, is predicted with reasonable accuracy, 15–20% lower than the measured value. The input data required in the model calculations are the compressive unnotched strength of the unidirectional plies and the in-plane fracture toughness K_{IC} of the plate. The fracture mechanics approach is justified because the microbuckled zone resembles a crack, and damage ahead of the microbuckle is small in extent compared to other specimen dimensions. Further experimental data for different biaxiality ratios and lay-ups are needed for the model validation.

Acknowledgments

This work was carried out with the financial support of the British Procurement Executive of the Ministry of Defence, Agreement SMCFU/654. The authors would like to thank P. T. Curtis and R. C. Dadey from the Structural Materials Centre, Defence and Evaluation Research Agency, Farnborough, for helpful discussions.

References

[1] Awerbuch, J., and Madhukar, M. S., "Notched Strength in Composite Laminates: Predictions and Experiments—A Review," *Journal of Reinforced Plastics and Composites*, Vol. 4, No. 3, 1985, pp. 3–159.

[2] Soutis, C., Curtis, P. T., and Fleck, N. A., "Compressive Failure of Notched Carbon Fibre Composites," *Proceedings of the Royal Society of London, Series A: Mathematical and Physical Sciences*, Vol. 440, No. 1909, 1993, pp. 241–256.

[3] Tutton, P. A., "The Effects of Specimen Geometry and Biaxial Loading on the Strength of Notched Carbon Fibre Composites," Cambridge Univ., TR, CUED/C/MATS/TR.96, Cambridge, England, U.K., Nov. 1982.

[4] Eftis, J., Jones, D. L., and Liebowitz, H., "Load Biaxiality and Fracture: Synthesis and Summary," *Engineering Fracture Mechanics*, Vol. 36, No. 4, 1990, pp. 537–574.

[5] Daniel, I. M., "Behaviour of Graphite/Epoxy Plates with Holes Under Biaxial Loading," *Experimental Mechanics*, Vol. 20, No. 1, 1980, pp. 1–8.

[6] Whitney, J. M., and Nuismer, R. J., "Stress Fracture Criteria for Laminated Composites Containing Stress Concentrations," *Journal of Composite Materials*, Vol. 8, July 1974, pp. 253–265.

[7] Soutis, C., and Fleck, N. A., "Static Compression Failure of Carbon Fibre T800/924C Composite Plate with a Single Hole," *Journal of Composite Materials*, Vol. 24, No. 5, 1990, pp. 536–558.

[8] Soutis, C., "Damage Tolerance of Open-Hole CFRP Laminates Loaded in Compression," *Composites Engineering*, Vol. 4, No. 3, 1994, pp. 317–327.

[9] Filiou, C., and Soutis, C., "Compression-Failure Modelling Under Biaxial Loading," Imperial College of Science, Technology, and Medicine, Progress Rept. TR.2-95, Agreement SMCFU/654, DRA, London, Oct. 1995.

[10] Filiou, C., and Soutis, C., "Stress Distributions Around Holes in Composite Laminates Subjected to Biaxial Loading," *Applied Composite Materials*, Vol. 5, No. 6, 1998, pp. 365–378.

[11] Lekhnitskii, S. G., *Anisotropic Plates*, Gordon and Breach, New York, 1968 (in Russian).

[12] Green, A. E., and Zerna, W., *Theoretical Elasticity*, Clarendon, Oxford, 1954.

[13] Green, A. E., and Taylor, G. I., "Stress Systems in Aeolotropic Plates, III," *Proceedings of the Royal Society of London, Series A: Mathematical and Physical Sciences*, Vol. 184, No. 997, 1945, pp. 181–195.

[14] Savin, G. N., *Stress Concentrations Around Holes*, Pergamon, Oxford, 1961.

[15] Konish, H. J., and Whitney, J. M., "Approximate Stresses in an Orthotropic Plate Containing a Circular Hole," *Journal of Composite Materials*, Vol. 9, April 1975, pp. 157–166.

[16] Soutis, C., "Failure of Notched CFRP Laminates Due to Fibre Microbuckling: A Topical Review," *Journal of the Mechanical Behaviour of Materials*, Vol. 6, No. 4, 1996, pp. 309–330.

[17] Guynn, E. G., Bradley, W. L., and Elber, W., "Micromechanics of Compression Failure in Open Hole Composite Laminates," *Composite Materials: Fatigue and Fracture*, American Society for Testing and Materials, STP 1012, Philadelphia, 1989, pp. 118–136.

[18] Waas, A. M., and Schultheisz, C. R., "Compressive Failure in Composites, Part II," *Progress in Aerospace Sciences*, Vol. 32, No. 1, 1995, pp. 43–78.

[19] Newman, J. C., Jr., "A Nonlinear Fracture Mechanics Approach to the Growth of Small Cracks," *AGARD Specialists Meeting on Behaviour of Short Cracks in Airframe Components*, AGARD, Sept. 1982, pp. 1–26.

[20] Tan, S. C., *Stress Concentrations in Laminated Composites*, Technomic, Lancaster, PA, 1994.

[21] Soutis, C., Curtis, P. T., and Fleck, N. A., "Compressive Failure of Notched Carbon Fibre Composites," *Proceedings of the Royal Society of London, Series A: Mathematical and Physical Sciences*, Vol. 440, No. 1909, 1993, pp. 241–256.

[22] Fleck, N. A., "Composite Failure of Fibre Composites," *Advances in Applied Mechanics*, edited by J. W. Hutchinson and T. Y. Wu, Vol. 34, Academic, New York, 1997, pp. 43–118.

[23] Sutcliffe, M. P. F., and Fleck, N. A., "Microbuckle Propagation in Fibre Composites," *Acta Metallurgica and Materialia*, Vol. 45, No. 3, 1997, pp. 921–932.

[24] Khamseh, A., and Waas, A. M., "Failure Mechanisms of Composite Plates with a Circular Hole Under Remote Biaxial Planar Compressive Loads," *Journal of Materials and Technology*, Vol. 119, Jan. 1997, pp. 56–64.

G. A. Kardomateas
Associate Editor